Research Article

iMedPub Journals
www.imedpub.com

Archives in Chemical Research
ISSN 2572-4657

2018
Vol.2 No.2:18

DOI: 10.21767/2572-4657.100018

Molecular Spectroscopic Investigations of (E)-1-(4 Methylbenzylidene) Urea Using DFT Method

Hannah Evangalin J[1], Bharanidharan S[2] and Dhandapani A[3]

1 Department of Physics, PRIST University, Chennai Campus, Mahabalipuram-603 102, Tamil Nadu, India

2 Department of Physics, Bharath Institute of Higher Education and Research, Bharath University, Chennai-600 073, Tamil Nadu, India

3 Department of Chemistry, CK College of Engineering and Technology, Cuddalore-607 003, Tamil Nadu, India

***Corresponding author:** Bharanidharan S

bharani.dharan0@gmail.com

Department of Physics, Bharath Institute of Higher Education and Research, Bharath University, Chennai-600 073, Tamil Nadu, India.

Tel: +91 9843225234

Citation: Evangalin JH, Bharanidharan S, Dhandapani A (2018) Molecular Spectroscopic Investigations of (E)-1-(4 Methylbenzylidene) Urea Using DFT Method. Arch Chem Res. Vol.2 No.2:18

Abstract

(E)-1-(4-methylbenzylidene)urea (EMBU) molecule has been synthesized and characterized by using FT-IR, FT-Raman and NMR spectral techniques. The quantum chemical calculations of EMBU have been done by using DFT/B3LYP/6-31G(d,p) basis set. The bond parameters were calculated at same level of theory. The vibrational assignment of EMBU is assigned precisely with the help of potential energy distributions (PED). The hyperconjugative stabilizing interactions are studied by the natural bonding orbital (NBO) analysis. The NLO activity of EMBU is calculated and compared with the reference Urea molecule. The active sites were identified by the molecular electrostatic potential mapped surface. In addition, Mulliken atomic charges and thermodynamic properties were calculated and analyzed.

Keywords: DFT; FT-IR; FT-Raman; PED; NMR; NLO

Received: February 02, 2018; **Accepted:** February 28, 2017; **Published:** December 03, 2018

Introduction

Schiff base compounds have been derived from aromatic amines and aromatic aldehydes. Schiff-base compounds exhibit a wide range of biological activities [1], anti-HIV [2], anti-tumor activities [3] and the transition metal complexes [4,5]. Very often it undergoes a variety of chemical reactions, being as a key precursor for new compounds exhibiting diverse molecular structures and properties [6,7]. It is worth mentioning that the salicylaldehyde moiety appears in many compounds exhibiting various biological activity, including reactants used in the design of compounds exhibiting anti-viral activity [8], as well as in reactions resulting in new compounds with anti-cancer [9,10] or anti-microbial activity [11]. It is also present during the synthesis of new products called “aspirin-like molecules” exhibiting anti-inflammatory activity [12].

The computational techniques are recently very useful in exploring nonlinear properties theoretically in useful manner. The simultaneous researches in the field of nonlinear materials have influenced the development of efficiencies of organic molecules as NLO material, since organic NLO materials often employ materials and device structures that have direct application to light multiplication.

In our present investigation we have focused on a simple organic molecule (E)-1-(4-methylbenzylidene) urea. We planned to investigate the nonlinear property of that molecule theoretically using first hyperpolarizability calculation. In addition to that, the vibrational spectral studies, NBO analysis, MEP surface and energy gap of the molecule are studied and discussed in detail.

Experimental Details

Synthesis of (E)-1-(4-Methylbenzylidene)urea

Equimolar amount of 4-methylbenzaldehyde and urea were dissolved in 30 ml of absolute ethanol. The mixture was shaken to make homogenous solution. Few drops of catalyst acetic acid were added to increase the rate of reaction. The content was refluxed at 90°C for 3 hours. The completion of the reaction was

monitored by thin layer chromatography. After the reaction was completed, the content was cooled the mixture was poured into water. The solid product obtained was filtered and purified using absolute ethanol

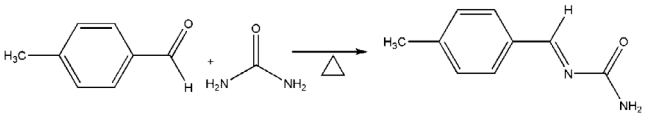

(E)-1-(4-methylbenzylidene)urea

Spectral Measurements

FT-IR, FT-Raman and NMR Spectrum: The FT-IR spectrum of the synthesized EMBU molecule was measured in the Mid-IR (4000–400 cm^{-1}) region at the spectral resolution of 4 cm^{-1} using on SHIMADZU FT-IR affinity Spectrophotometer (KBr pellet technique) in Faculty of Marine Biology, Annamalai University, Parangipettai. The FT-Raman spectrum was recorded on BRUKER: RFS27 spectrometer operating at laser 100mW in the spectral range of 4000–50 cm^{-1}. FT-Raman spectral measurements were carried out from SAIF, IIT, Chennai. NMR spectral studies were carried out using Bruker 400 MHz spectrometer, using TMS as an internal standard and DMSO-d6 as solvent and recorded at Annamalai University, Annamalainagar, Chidambaram. The ^{1}H and ^{13}C-NMR spectrum were shown in **Figure 1.**

Computational Details

The quantum chemical calculations were performed at DFT method with B3LYP/6-31G(d,p) basis set using Gaussian 03W [13] program package, invoking gradient geometry optimization [13,14]. The optimized structural parameters were used in the vibrational frequency calculations at the DFT level to characterize all the stationary points as minima. The vibrational modes were assigned on the basis of PED analysis using VEDA4 program package [15]. The Raman activity was calculated by using Gaussian 03W package and the activity was transformed into

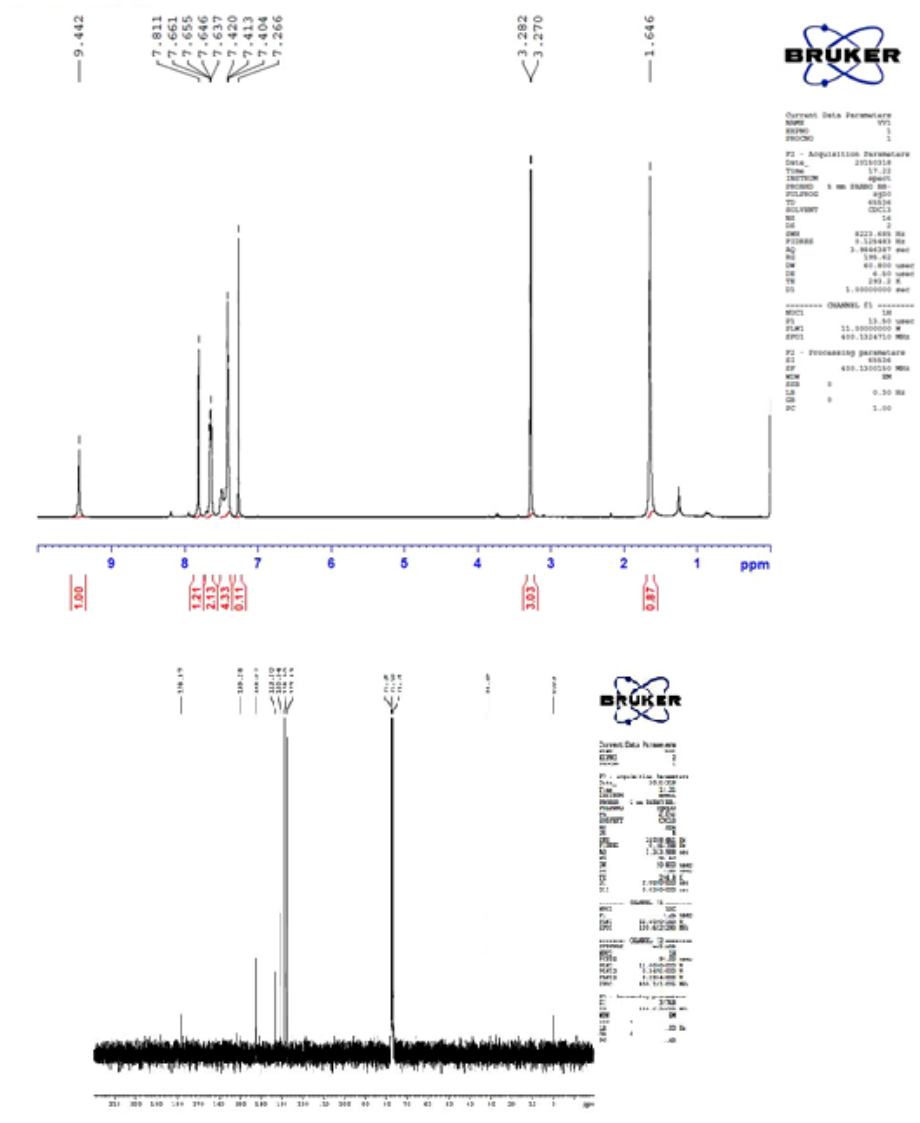

Figure 1 The ^{1}H and ^{13}C-NMR spectra of EMBU.

Raman intensity using Raint program [16] by the expression:

$$I_i = 10^{-12} \times (\nu_0 - \nu_i)^4 \times \frac{1}{\nu_i} \times RA_i \quad (1)$$

Where Ii is the Raman intensity, RAi is the Raman scattering activities, vi is the wavenumber of the normal modes and ν_0 denotes the wavenumber of the excitation laser [17].

Results and Discussion

Molecular geometry

The Optimized structure of EMBU molecule is shown in **Figure 2** with atom numbering scheme. The bond parameters such as bond lengths, bond angles and dihedral angles are calculated by DFT/B3LYP/6-31G(d,p) basis set and are listed in **Table 1**. In this case, the bond length of C-C and C-H are calculated around 1.40 and 1.08 Å, respectively. The bond lengths of related molecule was observed at C-C and C-H values are 1.38, 1.09 Å, respectively [18]. The carbonyl group bond C_{13}=O_{18} is appeared as π bond character; its bond length value is calculated about 1.2182 Å. Similarly, the π bond character of C=O is observed at 1.212 Å [19], which nearly coincides with calculated value. The σ and π bond characters of N_{12}-C_{13} and C_{11}=N_{12} are calculated as 1.4341 and 1.281Å are positively deviated with related molecule data (1.348 Å and 1.273 Å) data [19].

The bond angles of N_{12}-C_{13}-O_{18} and N_{14}-C_{13}=O_{18} is calculated about 126.06 and 123.77°, respectively. Similarly, the reported molecule calculated the bond angle value of N-C=O is 123.36°, which nearly matches with calculated values [18]. These results fairly explore that, during the course of rotation of the bond to the entire molecule gets disturbed and the properties of the molecule also changes. From the literature [20] and our theoretical investigation, the optimized structure is more stable.

Vibrational assignments

The EMBU molecule belongs to C_1 point group symmetry. It consists of 22 atoms and 60 normal modes of vibrations. The harmonic wavenumbers are calculated using B3LYP/6-31G(d,p) basis set and compared with recorded vibrational frequencies of FT-IR and FT-Raman spectra, respectively. Some discrepancies could be identified in between harmonic and observed frequencies, which are scaled down by proper scale factor [21,22]. The vibrational assignments are given in **Table 2**. The recorded and simulated FT-IR and FT-Raman spectra of EMBU are shown in **Figures 3** and **4**.

C=O Vibrations: The C=O stretching vibrations have been most extensively studied by IR and Raman spectroscopy. This multiply bonded group is highly polar and therefore gives rise to an intense IR absorption band, because of the different electro negativities are distributed between the two atoms [23]. The lone pair oxygen atom also determines the nature of the carbonyl group. In this study, the weak bands observed at 1672 and 1648 cm^{-1} in FTIR and FT-Raman spectra are assigned to C=O stretching vibration and its corresponding harmonic value lies at 1692 cm^{-1} (mode no: 11). This vibrational assignment is further supported by PED 88%.

C-C Vibrations: Generally, the phenyl ring carbon-carbon (C-C) stretching vibrations are observed in the region of 1625-1590, 1590-1575, 1540-1470, 1465-1430 and 1380-1280 cm^{-1} by Varsanyi (1974) [24]. In the present study, the FT-Raman bands observed at 1539 and FTIR band observed at 1598 cm^{-1} and are assigned to C-C stretching vibrations and their corresponding harmonic values appeared in the range of 1583 and 1541 cm^{-1} (mode nos: 13 and 14). These assignments are good agreement with literature [25].

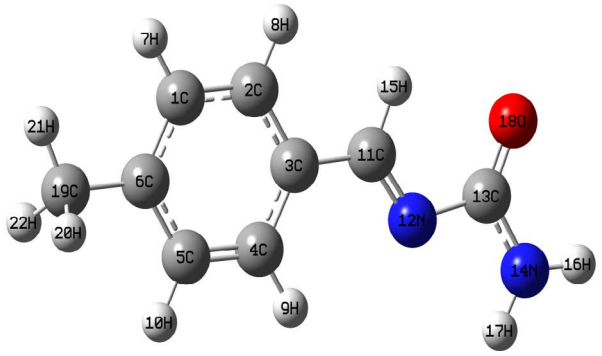

Figure 2 The optimized molecular structure of (E)-1-(4-methylbenzylidene)urea (EMBU).

The C-C in-plane bending vibrations observed at 1174 cm^{-1} in Raman and 613 cm^{-1} in IR spectrum and its corresponding calculated value appeared at 1182 and 623 cm^{-1} (mode no: 26 and 44). The $\Gamma C_4C_3C_5H_9$ mode predicted at 962 cm^{-1} (mode no: 34) is in agreement with IR band observed at 950 cm^{-1} with the help of PED 81%.

C-H Vibrations: In General, the CH stretching modes are expected to occur in the range 3200-2900 cm^{-1} [26,27]. In our study, C-H vibrations are observed at 3061, 2987 and 2929 cm^{-1} in FTIR spectrum. The corresponding harmonic frequencies lies at 3056, 2989 and 2936 cm^{-1} (mode nos: 4, 7 and 9) are belong to the same mode. These results were good agreement with experimental value with PED >95%. In benzene like molecule the C-H in-plane bending vibrations are appeared in the region 1000-1300 cm^{-1} and are usually weak intense. In our study, the frequency of the βCH vibrations are calculated in the region of 1438-1290 cm^{-1} (mode nos: 16 and 22) for this molecule. These modes are observed in the FTIR: 1298 cm^{-1}/FT-Raman: 1468 cm^{-1} spectra with weak intensity. The harmonic frequencies in the range 962 cm^{-1} (mode nos: 34) and FTIR band observed at 950 cm^{-1} assigned to ΓCH mode. These assignments are find support from PED.

N-H Vibrations: In general, the N-H stretching vibrations observed in the region 3400-3200 cm^{-1} [28]. In the present case, the N-H band assigned at 3460 cm^{-1} (mode no: 2). This assignment is further justified on the basis of their calculated PED value (100 %). The calculated wavenumber for β_{N-H} (1534 cm^{-1}/ mode no: 15) and Γ_{N-H} (585 cm^{-1}/ mode no: 45) modes well reproduced the experimental ones in FT-IR (1506 cm^{-1}) and FT-Raman (546 cm^{-1}) spectra with PED values (83% and 93%), respectively.

C-N Vibrations: The assignment of C=N stretching frequency is a rather difficult task since there are problems in identifying these

Table 1 The optimized bond parameters of EMBU.

Bond Lengths (Å)	B3LYP/6-31G(d,p)	Bond Angles (°)	B3LYP/6-31G(d,p)	Dihedral Angles (°)	B3LYP/6-31G(d,p)
R(1,2)	1.3921	A(2,1,6)	120.8487	D(6,1,2,3)	0.0032
R(1,6)	1.3973	A(2,1,7)	119.6136	D(6,1,2,8)	179.9973
R(1,7)	1.0848	A(6,1,7)	119.5377	D(7,1,2,3)	-179.994
R(2,3)	1.4003	A(1,2,3)	120.6796	D(7,1,2,8)	-0.0001
R(2,8)	1.0853	A(1,2,8)	119.8559	D(2,1,6,5)	-0.0096
R(3,4)	1.4055	A(3,2,8)	119.4645	D(2,1,6,19)	179.957
R(3,11)	1.4605	A(2,3,4)	118.6712	D(7,1,6,5)	179.9879
R(4,5)	1.3847	A(2,3,11)	119.2354	D(7,1,6,19)	-0.0456
R(4,9)	1.083	A(4,3,11)	122.0934	D(1,2,3,4)	0.003
R(5,6)	1.4056	A(3,4,5)	120.3294	D(1,2,3,11)	179.9981
R(5,10)	1.0856	A(3,4,9)	118.7107	D(8,2,3,4)	-179.991
R(6,19)	1.5076	A(5,4,9)	120.9599	D(8,2,3,11)	0.004
R(11,12)	1.281	A(4,5,6)	121.223	D(2,3,4,5)	-0.0026
R(11,15)	1.0958	A(4,5,10)	119.5125	D(2,3,4,9)	179.9914
R(12,13)	1.4341	A(6,5,10)	119.2645	D(11,3,4,5)	-179.998
R(13,14)	1.3596	A(1,6,5)	118.2481	D(11,3,4,9)	-0.0036
R(13,18)	1.2182	A(1,6,19)	121.3126	D(2,3,11,12)	-179.999
R(14,16)	1.0061	A(5,6,19)	120.4392	D(2,3,11,15)	0.0028
R(14,17)	1.0058	A(3,11,12)	123.1686	D(4,3,11,12)	-0.0038
R(19,20)	1.0945	A(3,11,15)	116.9094	D(4,3,11,15)	179.9978
R(19,21)	1.0914	A(12,11,15)	119.922	D(3,4,5,6)	-0.004
R(19,22)	1.0944	A(11,12,13)	115.0758	D(3,4,5,10)	179.9926
		A(12,13,14)	110.1617	D(9,4,5,6)	-179.998
		A(12,13,18)	126.0669	D(9,4,5,10)	-0.0012
		A(14,13,18)	123.7714	D(4,5,6,1)	0.01
		A(13,14,16)	119.3699	D(4,5,6,19)	-179.957
		A(13,14,17)	119.9243	D(10,5,6,1)	-179.987
		A(16,14,17)	120.7058	D(10,5,6,19)	0.0466
		A(6,19,20)	111.0369	D(1,6,19,20)	-119.878
		A(6,19,21)	111.4884	D(1,6,19,21)	0.5522
		A(6,19,22)	111.0578	D(1,6,19,22)	121.0241
		A(20,19,21)	107.9612	D(5,6,19,20)	60.0881
		A(20,19,22)	107.1337	D(5,6,19,21)	-179.482
		A(21,19,22)	107.983	D(5,6,19,22)	-59.0101
				D(3,11,12,13)	-179.998
				D(15,11,12,13)	0.0003
				D(11,12,13,14)	-179.996
				D(11,12,13,18)	0.0049
				D(12,13,14,16)	179.9973
				D(18,13,14,17)	-179.998

Table 2 The fundamental vibrational assignments of EMBU.

Mode	Theoretical		Experimental		IR Int[b]	Raman Int[c]	Vibrational Assignments PED≥(10%)[d]
No	Un Scaled	Scaled[a]	IR	Raman			
1	3745	3603	3606		16.8	0.9	vN14H16(100)+vN14H17(100)
2	3608	3471	3460		20.4	2.5	vN14H16(100)+vN14H17(100)
3	3199	3077			0.7	1.4	vC4H9(95)
4	3177	3056	3061		3.8	3.2	vC1H7(97)+vC2H8(95)
5	3160	3040			1.6	1.8	vC1H7(97)+vC2H8(95)
6	3160	3040			4.3	1.5	vC5H10(89)
7	3107	2989	2987		4.6	1.6	vC19H21(99)
8	3074	2957			3.5	2.7	vC19H20(90)+vC19H22(90)

9	3052	2936	2929		2.8	1.1	νC11H15(100)
10	3025	2910			6.8	9.8	νC19H20(90)+νC19H21(99)+νC19H22(90)
11	1762	1695	1672	1648	111.6	1.5	νO18C13(88)
12	1671	1607			52.2	33.9	νN12C11(66)
13	1646	1583	1598		45.4	100	νC4C5(53)+νC2C1(62)+νC2C3(48)
14	1602	1541		1539	0.4	0.9	νC4C3(47)+νC6C5(79)+βH16N14H17(83)+βC2C1C6(57)
15	1595	1534	1506		117.4	27.1	βH16N14H17(83)
16	1543	1484		1468	0.9	3.5	βH7C1C2(54)+βH9C4C5(66)+βH10C5C4(75)+βC4C 3C2(65)
17	1494	1438	1435		4.5	4.9	βH21C19C6(76)+βH20C19H22(84)
18	1486	1429			2.1	1.4	βH20C19C6(85)+ΓC19H20C6H21(91)
19	1440	1385			4.5	2.9	νC4C5(53)+νC2C1(62)
20	1415	1361	1354		0.4	4.4	βH20C19H22(84)+ΓC19H21H22H20(80)
21	1400	1347			18.4	2.8	νN12C11(66)+βH15C11N12(82)
22	1341	1290	1298		28.1	2.4	νN14C13(55)+βH9C4C5(66)+βH10C5C4(75)
23	1338	1287			0.7227	1.3	νC2C3(48)+νC6C5(79)
24	1325	1275			100	15	νN14C13(55)+βH16N14C13(56)+βH15C11N12(82)
25	1246	1199			31.2	30	νC11C3(50)+βH7C1C2(54)+βH10C5C4(75)+βH15C1 1N12(82)
26	1229	1182		1174	3.9	9.6	νC2C1(62)+βC1C6C5(51)+νC19C6(64)
27	1198	1152			19.8	22.5	βH7C1C2(54)+βH8C2C1(50)+βH9C4C5(66)+βH10C 5C4(75)
28	1138	1095			1.7	1.1	νC4C5(53)+νC2C1(62)+βH7C1C2(54)+βH8C2C1(50)+βH9 C4C5(66)
29	1098	1056			1.1	8.5	νO18C13(88)+νN14C13(55)+βH16N14C13(56)
30	1061	1021			1.5	0	βH20C19C6(85)+ΓC19H20C6H21(91)
31	1053	1013	1002	1009	0.9	0.9	τH15C11N12C13(82)
32	1035	996			2.3	0.3	βC1C6C5(51)+βC2C1C6(57)+βC6C5C4(57)
33	1008	969			4.1	0.6	νC6C5(79)+βH21C19C6(76)
34	999	962	950		0	0	ΓC4C3C5H9(81)+τH10C5C4C3(85)
35	971	934			0.1	0	τH7C1C2H8(77)
36	935	899			31	4.6	νN12C13(51)+βN12C11C3(75)
37	874	840	867		0	6.8	νC2C3(48)+νC4C3(47)+νC11C3(50)
38	856	824	829		0.9	0	τH7C1C2C3(82)+ΓC4C3C5H9(81)+τH10C5C4C3(85)
39	838	806			11	0	τH7C1C2C3(82)+τH10C5C4C3(85)
40	786	756			0.2	6.6	νC19C6(64)+βC4C3C2(65)
41	780	750	746		0.1	0	τC3C11N12C13(68)+ΓO18N12N14C13(70)
42	723	695			1.3	0.2	τC1C6C2C3(82)+τC3C2C4C5(83)+τC1C6C4C5(77)
43	657	632			1.9	1.6	νC6C5(79)+βN12C13O18(65)+βC6C5C4(57)
44	647	623	613		3.6	2.9	βC1C6C5(51)+βN12C13O18(65)
45	608	585		546	0.2	0	ΓH16N14C13N12(93)
46	563	542			1	0.8	βN12C11C3(75)+βN14C13N12(80)+βC2C3C11(68)
47	512	492			8.7	0.1	τC3C2C4C5(83)+τC1C6C4C5(77)
48	509	489	476		3.4	0.2	βC1C6C5(51)+βN14C13N12(80)
49	422	406			0.1	0.1	τC1C6C2C3(82)+τC1C6C4C5(77)
50	371	357			1.6	0.8	βN14C13N12(80)+βC2C3C11(68)+βC5C6C19(75)
51	352	339			0.9	1.4	τC3C2C4C5(83)+τC4C5C6C19(68)+τC1C2C3C11(79)
52	298	287			0.5	1.8	βN14C13N12(80)+βC2C3C11(68)+βC5C6C19(75)
53	240	231			1.2	3.2	νC11C3(50)+βN12C13O18(65)+βC4C3C2(65)+βC13N1 2C11(61)
54	230	221			61	0.5	ΓN14H16C13H17(89)
55	189	182			0	0.8	τC4C3C11N12(77)+τC3C2C4C5(83)+τC4C5C6C19(68)
56	151	146		132	0.9	0.3	τC4C3C11N12(77)+τN14C13N12C11(95)+τC3C11N1 2C13(68)
57	94	91		101	0.3	2.6	βN12C11C3(75)+βC2C3C11(68)+βC13N12C11(61)

58	63	60		63	0	2.2	τC3C11N12C13(68)+τC1C2C3C11(79)
59	32	31			2.3	1.5	τC4C3C11N12(77)+τN14C13N12C11(95)
60	15	15			0	22.8	τH22C19C6C5(91)

v: Stretching, β: in-plane-bending, Γ: out-of-plane bending, τ: Torsion,
[a] Scaling factor: 0.9620,
[b] Relative IR absorption intensities normalized with highest peak absorption equal to 100,
[c] Relative Raman intensities normalized to 100,
[d] Potential energy distribution calculated at B3LYP/6-31G(d,p) level.

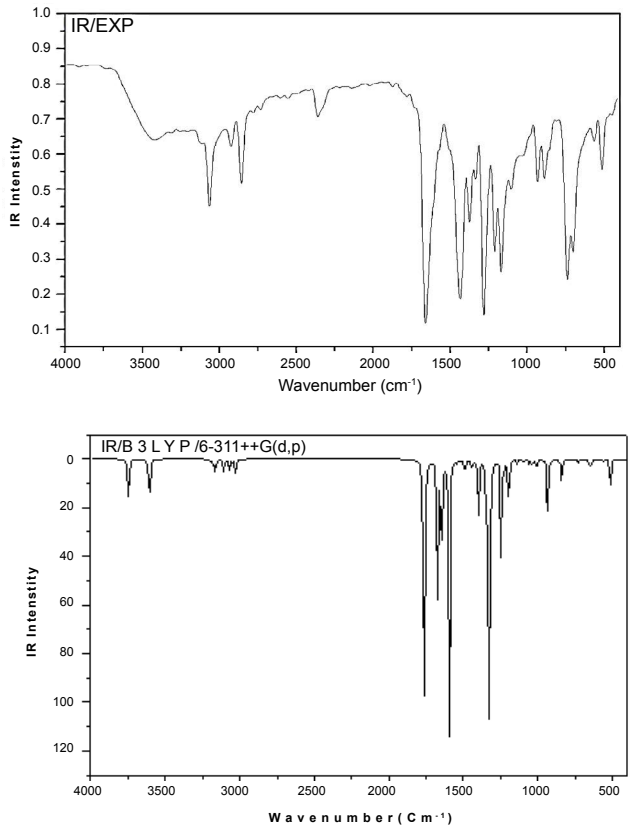

Figure 3 The combined Theoretical and Experimental IR spectra of EMBU.

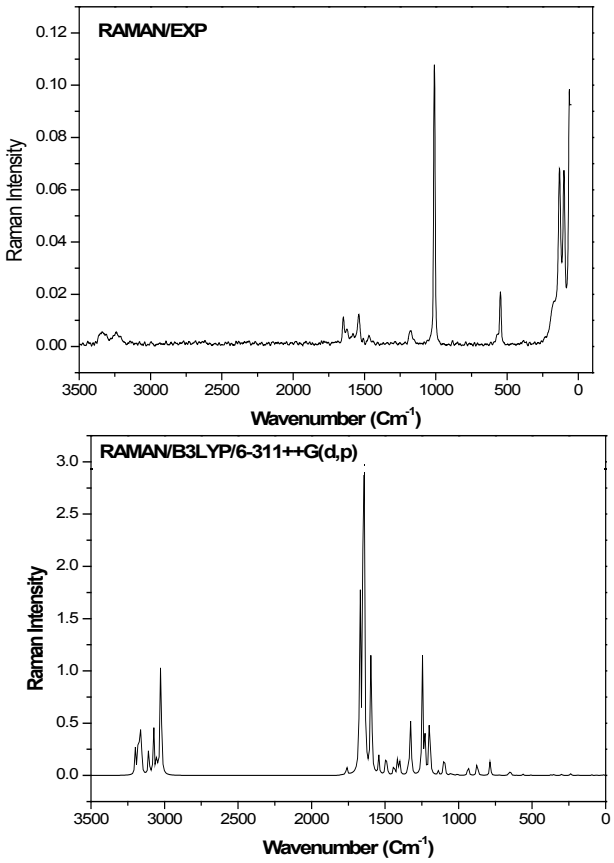

Figure 4 The combined Theoretical and Experimental FT-Raman spectra of EMBU.

frequencies from other vibrations. The ring C–N vibrations are appeared in the region 1650–1550 cm^{-1} [29]. The bands obtained at 1598 cm^{-1} in FT-IR and at 1539 cm^{-1} in FT-Raman spectra have been assigned to C=N stretching vibrations of title molecule. The corresponding theoretical wavenumber lies at 1583 and 1541 cm^{-1}, which is comparable to experimental wavenumber with PED contribution ≥ 45%. Silverstein et al., [30] assigned C–N stretching vibrations occurred in the region 1382–1266 cm^{-1} for the aromatic amines. The C-N stretching vibrations of title molecule were obtained at 1298 cm^{-1} in FT-IR spectrum. The band calculated at 1290 cm^{-1} from DFT is assigned to C-N stretching vibration of the present molecule.

NLO property

In this study, the electronic dipole moment, molecular polarizability, anisotropy of polarizability and molecular first hyperpolarizability of EMBU were calculated at DFT/B3LYP/6-31G(d,p) basis set and are presented in **Table 3**. It is well-known that the higher values of dipole moment, molecular polarizability, and hyperpolarizability which enhances the NLO property. Urea is one of the prototypical molecule used in the study of the NLO property of molecular systems, and thus, it was used frequently as a threshold value for comparative purposes. The first hyperpolarizability value of EMBU was calculated as 10.595 × 10^{-30} esu. According to these result, the β_0 value of present molecule is twenty-eight times larger than the magnitude of urea, which implies that the title molecule might become a kind of good NLO material.

NBO analysis

The NBO analysis provides an efficient method for studying intra-

Table 3 The NLO measurements of EMBU.

Parameters	B3LYP/6-31G(d,p)
Dipole moment (μ)	**Debye**
μ_x	-1.1362
μ_y	-0.8895
μ_z	0.0003
μ	1.4429 Debye
Polarizability (α_0)	***x10^{-30}esu***
α_{xx}	214.95
α_{xy}	-4.99
α_{yy}	125.77
α_{xz}	-0.02
α_{yz}	0.00
α_{zz}	70.94
α_0	3.1476x10^{-30}esu
Hyperpolarizability (β_0)	***x10^{-30}esu***
β_{xxx}	1383.41
β_{xxy}	211.90
β_{xyy}	-151.05
β_{yyy}	30.28
β_{xxz}	0.10
β_{xyz}	0.09
β_{yyz}	-0.25
β_{xzz}	-24.15
β_{yzz}	-31.28
β_{zzz}	0.19
β_0	10.595x10^{-30}esu

Standard value for urea (μ=1.3732 Debye, β_0=0.3728x10^{-30}esu)

and inter-molecular bonding and interaction among bonds, and also provides a convenient basis for investigating charge transfer or conjugative interaction in molecular systems [31].

In this present study, the NBO analysis has been carried out with DFT/B3LYP/6-31G(d,p) level of basis set and which deals the intra-molecular charge transfer within the molecule. In any molecule, the π character of the bond plays an important role when compare with σ bond character. In such a way that this molecule delivers maximum delocalization energy during the transition between π and π* bond whereas the ED of the donor (Lewis) bond decreases with increasing of ED of acceptor (Non-Lewis) bonds. In our case, the conjugative π bonds in the phenyl ring shows maximum delocalization during the interaction with π* acceptor bonds. It is evident from our title compound that the energy transfer from πC_1-C_6 to $\pi^* C_2$-C_3, πC_4-C_5 to $\pi^* C_1$-C_6 and πC_2-C_3 to $\pi^* C_{11}$-N_{12} are reveals the hyperconjucative energy about 97.74, 92.51 and 86.69 KJ/mol, respectively. Similarly, the lone pair atoms such as oxygen and nitrogen also transfer more energy to donor and acceptor bonds. The LP(1)N14 to C13-O18 and LP(2)O18 to N12-C_{13} bonds transfer the energy about 252.71 and 106.78 KJ/mol, respectively. The NBO donor and acceptor orbital interactions of EMBU are listed in **Table 4**. The maximum hyperconjugative $E^{(2)}$ energy of lone pair atoms during the intra-molecular interaction, which leads the molecule towards medicinal and biological applications.

HOMO-LUMO analysis

The HOMO and the LUMO are called frontier molecular orbitals as they lie at the outermost boundaries of the electrons of the molecules. The HOMO and LUMO are the main orbitals responsible for chemical stability. The HOMO–LUMO orbitals of the EMBU are as shown in **Figure 5**. The calculated values of the HOMO and LUMO energies and band gap energy are listed in **Table 5**. The positive and negative phases are represented in green and red color, respectively. HOMO represents the electron-donating ability of a molecule, whereas LUMO indicates its ability to accept electrons. The frontier orbital gap helps to characterize the chemical reactivity and kinetic stability of the molecule. In the present study, the energy gap have been calculated using B3LYP/6-31G(d,p) level are 4.76415 eV. This small energy gap is associated with high chemical reactivity and low kinetic stability.

MEP analysis

The MEP surface map was calculated at B3LYP/6-31G(d,p) method. It is very useful descriptor in understanding the sites for electrophilic and nuleophilic as well as hydrogen bonding

Table 4 The natural bond orbital analysis of EMBU.

Type	Donor (i)	ED/e	Acceptor (j)	ED/e	$E^{(2)}$ KJ/mol	E(j)-E(i) a.u.	F(i,j) a.u.
π -π*	C_1–C_6	1.6378	C_2–C_3	0.3732	97.74	0.28	0.072
π -π*			C_4–C_5	0.2690	69.12	0.29	0.063
π -σ*			C_{19}–H_{20}	0.0084	10.96	0.65	0.041
π -σ*			C_{19}–H_{22}	0.0083	10.75	0.65	0.04
π -π*	C_2–C_3	1.6299	C_1–C_6	0.3264	73.43	0.29	0.064
π -π*			C_4–C_5	0.2690	81.46	0.29	0.068
π -π*			C_{11}–N_{12}	0.1315	86.69	0.28	0.072
π -π*	C_4–C_5	1.6794	C_1–C_6	0.3264	92.51	0.29	0.071
π -π*			C_2–C_3	0.3732	75.06	0.28	0.065
π -π*	C_{11}–N_{12}	1.8898	C_2–C_3	0.3732	32.64	0.35	0.05
π -π*			C_{13}–O_{18}	0.3259	86.02	0.35	0.08
π -π*	C_{13}–O_{18}	1.9906	C_{11}–N_{12}	0.1315	8.54	0.38	0.026
π -π*			C_{13}–O_{18}	0.3259	6.86	0.38	0.024
n -σ*	LP(1) N_{12}	1.9205	C_3–C_{11}	0.0316	7.7	0.85	0.036
n -σ*			C_{11}–H_{15}	0.0401	44.06	0.77	0.081
n -σ*			C_{13}–N_{14}	0.0661	8.41	0.84	0.037
n -σ*			C_{13}–O_{18}	0.0234	38.07	0.99	0.086
n -π*	LP(1) N_{14}	1.7415	C_{13}–O_{18}	0.3259	252.71	0.28	0.119
n -σ*	LP(1) O_{18}	1.9775	N_{12}–C_{13}	0.0885	9.79	1.07	0.045
n -σ*			C_{13}–N_{14}	0.0661	8.54	1.15	0.044
n -σ*	LP(2) O_{18}	1.8497	N_{12}–C_{13}	0.0885	106.78	0.63	0.115
n -σ*			C_{13}–N_{14}	0.0661	97.61	0.71	0.117

*$E^{(2)}$ means energy of hyperconjugative interactions,
LP = Lone pair (non-bonding molecular orbital)

interactions [32]. The importance of MEP lies in the fact that it simultaneously displays molecular size, shape as well as positive, negative and neutral electrostatic potential regions in terms of colour grading as shown in **Figure 6**. Potential increases in the order red < orange < yellow < green < blue. The colour code of these maps, where blue indicates the strongest interaction and red indicates the strongest repulsion. In this study, the negative region is located over the carbonyl group and the positive region is located over Hydrogen atom in the imine linkage.

Mulliken charges

Mulliken populations can be used to characterize the electronic charge distribution in a molecule and the bonding, anti-bonding, or non-bonding nature of the MOs for pair of atoms [33]. Mulliken atomic charge calculation has an important role in the application of quantum chemical calculation to molecular system. The total atomic charges of EMBU are calculated by Mulliken population analysis with DFT method B3LYP/6-31G(d,p) basis set are listed in **Table 6**. The Mulliken atomic charge plot for EMBU is plotted in **Figure 7**. The most positive charges calculated at C3/0.636162 and C6/0.651105 in the present molecule. The C_6 atom has high positive charge due to the attachment of methyl group. Similarly, the negative charges were calculated at C1/-0.764424 and C19/-0.612242, respectively. From the results, C_1 atom shows the higher negative charge due to the presence aromatic ring. The nitrogen and oxygen atoms also be a negative charge such as N12/-0.118445, N14/-0.393447 and O18/-0.362573, respectively.

Thermodynamic properties

The standard thermodynamic functions: heat capacity ($C^0_{p,m}$), entropy (S^0_m) and enthalpy changes (H^0_m) for the EMBU were calculated using DFT method at B3LYP/6-31G(d,p) basis set and are listed in **Table 7**. Therefore, it can be observed that these thermodynamic functions are increasing with temperature ranging from 100 to 1000 K due to the molecular vibrational intensities increase with temperature [34]. The correlation equations among thermodynamic functions due to the temperature were fitted by quadratic, linear and quadratic formula and the corresponding fitting factors (R^2) for these thermodynamic properties are 0.99957, 0.99997 and 0.99971. The corresponding fitting equations are as follows, and the correlation graphs are shown in **Figure 8**.

$C^0_{p,m} = -1.73055 + 0.1542T - 6.3237x10^{-5} T^2$ ($R^2 = 0.99957$)

$S^0_m = 3.06457 + 0.13745T - 1.83581x10^{-5} T^2$ ($R^2 = 0.99997$)

$\Delta H^0_m = 107.82213 + 0.00557T + 1.88572x10^{-5} T^2$ ($R^2 = 0.99971$)

All the thermodynamic data are supportive information for further study on the molecule.

Conclusion

The nonlinear optical analysis of EMBU has been carried out by quantum chemical calculations at DFT level. The bond parameters (bond lengths, bond angles and dihedral angles) are agree well with the related molecule XRD data. The observed and calculated wavenumbers of EMBU are well supported by the literature values. The hyperpolarizability (β_0) value of EMBU molecule is

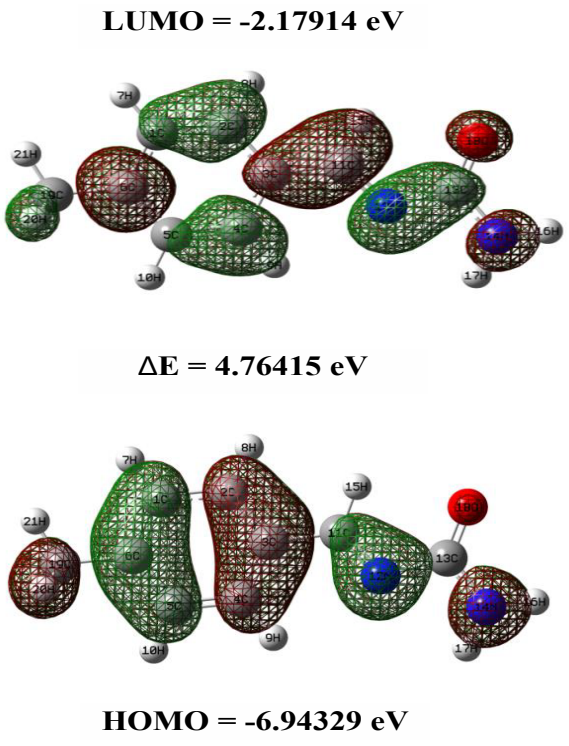

Figure 5 The frontier molecular orbitals of EMBU.

Table 5 The frontier molecular orbitals of EMBU.

Orbitals	Energy (a.u)	Energy (eV)
39O	-0.30489	-8.29636
40O	-0.279438	-7.60379
41O	-0.272717	-7.4209
42O	-0.258641	-7.03788
43O	-0.255165	-6.94329
44V	-0.080083	-2.17914
45V	-0.029496	-0.80262
46V	-0.012194	-0.33181
47V	-0.006217	-0.16917
48V	0.00296	0.080545

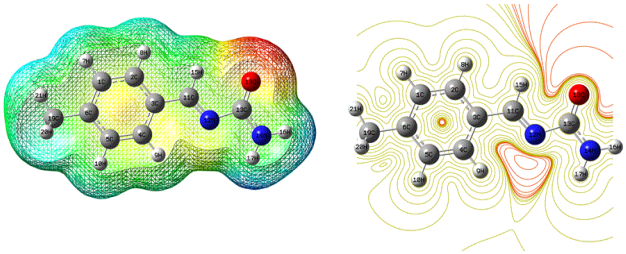

Figure 6 The MEP surface of EMBU.

calculated about 10.595x10^{-30} esu, which is twenty-eight times greater than that of standard urea. The NBO analysis reveals that, the charge transfer occur within the molecule and the maximum energy takes place during π-π* transition. The energy gap of EMBU molecule is calculated at 4.76415 eV, which leads the title molecule to become less stable and more reactive. The reactive sites of EMBU molecule is predicted by MEP surface. In addition, Mulliken atomic charges and thermodynamic properties are also calculated and analyzed.

Table 6 The Mulliken atomic charges of EMBU.

Atoms	Charges	Atoms	Charges
1C	-0.764424	12N	-0.118445
2C	-0.567188	13C	0.247575
3C	0.636162	14N	-0.393447
4C	-0.272493	15H	0.187019
5C	-0.251654	16H	0.30635
6C	0.651105	17H	0.266017
7H	0.138265	18O	-0.362573
8H	0.161024	19C	-0.612242
9H	0.179329	20H	0.159652
10H	0.176258	21H	0.152303
11C	-0.077157	22H	0.158565

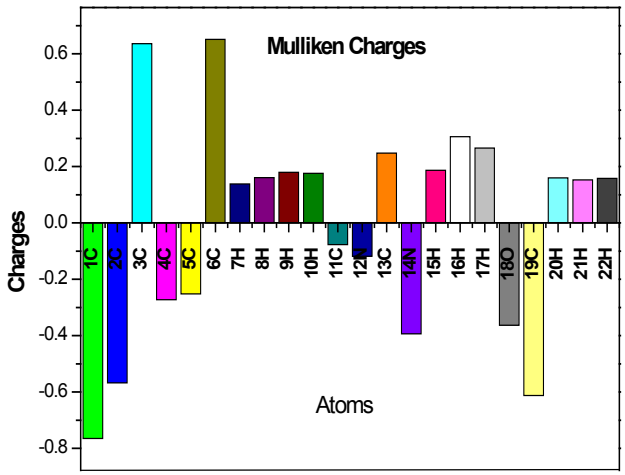

Figure 7 The Mulliken atomic charges plot of EMBU.

Table 7 Thermodynamic properties of EMBU at different temperatures.

T	S (J/mol.K)	Cp (J/mol.K)	ΔH (KJ/mol)
100	322.65	102.31	7.77
200	431.05	157.53	21.14
300	504.31	248.38	39.40
400	572.12	314.48	68.66
500	656.22	361.16	102.77
600	746.02	414.85	129.31
700	811.21	450.54	171.54
800	852.00	459.45	237.19
900	928.71	498.26	285.37
1000	981.74	523.05	335.81

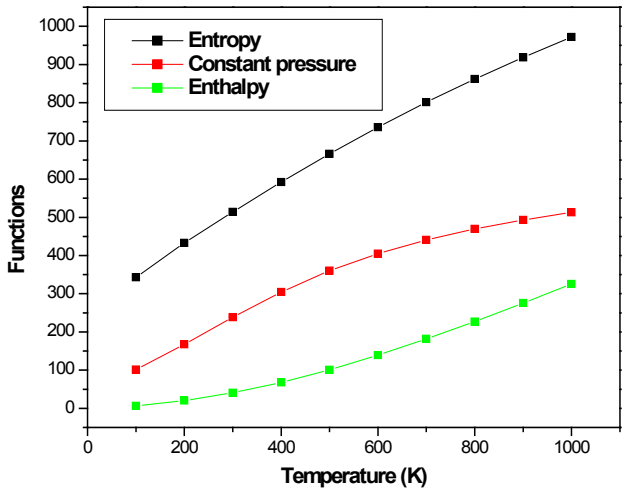

Figure 8 The thermodynamic properties of EMBU at different temperatures.

References

1 Karthikeyan MS, Prasad DJ, Poojary B, Bhat KS, Holla BS, et al. (2006) Synthesis and biological activity of Schiff and Mannich bases bearing 2,4-dichloro-5-fluorophenyl moiety. Bioorg Med Chem 14: 7482-7489.

2 Sriram D, Yogeeswari P, Sirisha N, Saraswat V (2006) Abacavir prodrugs: Microwave-assisted synthesis and their evaluation of anti-HIV activities. Bioorg Med. Chem Lett 16: 2127-2129.

3 Liu G, Peiliao J, Huang S, Lishen G, Qinyu R (2001) Fluorescence Spectral Study of Interaction of Water-soluble Metal Complexes of Schiff-base and DNA. Anal Sci 17: 1031-1035.

4 Khalaji AD, Hadadzadeh H, Gotoh K, Ishida H (2009) catena-Poly [[[N,N′-bis(3-methoxybenzylidene)ethylenediamine]copper(I)]-μ-thiocyanato-κ2N:S]. Acta Cryst 65: 70.

5 Morshedi M, Amirnasr M, Triki S, Khalaji AD (2009) New (NS)2 Schiff base with a flexible spacer: Synthesis and structural characterization of its first coordination polymer [Cu2(μ-I)2(μ-(thio)2dapte)]n (1). Inorg. Chim Acta 362: 1637-1640.

6 Sacconi L, Bertini I (1966) Complexes of Copper(II) with Schiff Bases Formed from Salicylaldehydes and N-Substituted Ethylenediamines. Inorg Chem 5: 1520-1522.

7 Sales ZS, Mani NS (2009) An Efficient Intramolecular 1,3-Dipolar Cycloaddition Involving 2-(1,2 Dichlorovinyloxy)aryldiazomethanes: A One-Pot Synthesis of Benzofuropyrazoles from Salicylaldehydes J Org Chem 74: 891-894.

8 Wang PH, Keck JG, Lien EJ, Lai MMC (1990) Design, synthesis, testing, and quantitative structure-activity relationship analysis of substituted salicylaldehyde Schiff bases of 1-amino-3-hydroxyguanidine tosylate as new antiviral agents against coronavirus. J Med Chem 33: 608-614.

9 Chinigo GM, Paige M, Grindrod S, Hamel E, Dakshanamurthy S, et al. (2008) Asymmetric synthesis of 2,3-dihydro-2-arylquinazolin -4-ones: methodology and application to a potent fluorescent tubulin inhibitor with anticancer activity. J Med Chem 51: 4620-4631.

10 Abd-Elzaher MM, Moustafa SA, Labib AA, Ali MM (2010) Synthesis, characterization and anticancer properties of ferrocenyl complexes containing a salicylaldehyde moiety. Monatsh Chem Chem Mon 141: 387-393.

11 Prisakar VI, Tsapkov VI, Buracheéva SA, Byrké MS, Gulya AP (2005) Synthesis and Antimicrobial Activity of Coordination Compounds of Copper with Substituted Salicylaldehyde Thiosemicarbazones. J Pharm Chem 39: 313-315.

12 Lazzarato L, Donnola M, Rolando B, Marini E, Cena C, et al. (2008) Searching for new NO-donor aspirin-like molecules: a new class of nitrooxy-acyl derivatives of salicylic acid. J Med Chem 51: 1894-1903.

13 Frisch MJ, Trucks GW, Schlegel HB, Scuseria GE, Robb MA, et al. (2004) Theoretical and Computational Aspects of Magnetic Organic Molecules. Gaussian Inc, Wallingford, USA.

14 Schlegel HB (1982) Optimization of equilibrium geometries and transition structures. J Comput Chem 3: 214-218.

15 Jamróz MH (2006) Vibrational modes of 2,6-, 2,7-, and 2,3-diisopropyl naphthalene. A DFT study. J Mol Struct 787: 172-183.

16 Michalska D (2003) Raint Program, Wroclaw University of Technology, Poland.

17 Michalska D, Wysokinski R (2005) The prediction of Raman spectra of platinum(II) anticancer drugs by density functional theory. Chem Phys Lett 403: 211-217.

18 Ramesh Babu N, Subashchandrabose S, Syed Ali Padusha M, Saleem H, Erdogdu Y (2014) Synthesis and spectral characterization of hydrazone derivative of furfural using experimental and DFT methods. Spectrochim Acta A 120: 314-322.

19 Song MZ, Fan CG (2009) (E)-N-(2-Furylmethylene)benzohydrazide. Acta Cryst E 65: o2800.

20 Araujo-Andrade C, Giuliano BM, Gómez-Zavaglia A, Fausto R (2012) Structure and UV-induced photochemistry of 2-furaldehyde dimethylhydrazone isolated in rare gas matrices. Spectrochim Acta A 97: 830-837.

21 Radom L, John A, Pople (1970) Molecular orbital theory of the electronic structure of organic compounds. IV. Internal rotation in hydrocarbons using a minimal Slater-type basis. J American Chem Soc 92: 4786-4795.

22 Pople JA, Scott AP, Wong MW, Radom L (1993) Scaling Factors for Obtaining Fundamental Vibrational Frequencies and Zero-Point Energies from HF/6-31G* and MP2/6-31G* Harmonic Frequencies. Israel J Chem 33: 345-350.

23 Dabbagh HA, Teimouri A, Chermahini AN, Shahraki M (2008) DFT and ab initio study of structure of dyes derived from 2-hydroxy and 2,4-dihydroxy benzoic acids. Spectrochim Acta A 69: 449-459.

24 Varasanyi G (1974) Assignments for Vibrational Spectra of Seven Hundred Benzene Derivatives, vol. 1–2, Adam Hilger.

25 Ravikumar C, Hubert Joe H, Jayakumar VS (2008) Charge transfer interactions and nonlinear optical properties of push–pull chromophore benzaldehyde phenylhydrazone: A vibrational approach. Chem Phy Lett 460: 552-558.

26 Rastogi V, Palafox MA, Tanwar RP, Mittal L (2002) 3,5-Difluorobenzonitrile: ab initio calculations, FT-IR and Raman spectra. Spectrochim. Acta A 58: 1987-2004.

27 Silverstein M, Basseller CG, Morill C (1981) Spectrometric identification of organic compound, JohnWiley; Network.

28 Lorenc J (2012) Dimeric structure and hydrogen bonds in 2-N-ethylamino-5-metyl-4-nitro-pyridine studied by XRD, IR and Raman methods and DFT calculations. Vib Spectrosc 61: 112-123.

29 Palafox MA, Nunez JL, Gil M (2002) Accurate scaling of the vibrational spectra of aniline and several derivatives. J Mol Struct 593: 101-106.

30 Silverstein M, Clayton Basseler G, Morill C (1981) Spectrometric Identification of Organic Compounds, Wiley, New York.

31 Snehalatha M, Ravikumar C, Hubert Joe I, Sekar N, Jayakumar VS (2009) Spectroscopic analysis and DFT calculations of a food additive Carmoisine. Spectrochim Acta A 72: 654-662.

32 Politzer P, Truhlar DG (1981) Chemical Applications of Atomic and Molecular Electrostatic Potentials.

33 Mulliken RS (1955) Electronic Population Analysis on LCAO–MO Molecular Wave Functions. J Chem Phys 23: 1833-1841.

34 Sajan D, Lynnette J, Vijayan N, Karabacak M (2011) Natural bond orbital analysis, electronic structure, non-linear properties and vibrational spectral analysis of l-histidinium bromide monohydrate: A density functional theory. Spectrochim Acta A 81: 85-98.